CONF-891007--25

DE90 001738

PARTICLE EXHAUST SCHEMES IN THE DIII-D ADVANCED DIVERTOR CONFIGURATION*

M. M. Menon and P. K. Mioduszewski

Oak Ridge National Laboratory, P.O. Box 2009, Oak Ridge, TN 37831-8072

ABSTRACT

For density control in long-pulse operation, the open divertor on the DIII-D tokamak will be equipped with a baffled chamber and a pumping system. The throat of the baffle chamber is sized to provide optimal pumping for the typical plasma equilibrium configuration. Severe limitations on the toroidal conductance of this baffle chamber require the use of in-vessel pumping to achieve the desired particle exhaust of about 25 Torr•l/s. Two separate pumping schemes are considered: an array of titanium getter modules based on the design developed by the Tore Supra team and a cryocondensation pump. The merits and demerits of each scheme are analyzed, and the design considerations introduced by the tokamak environment are brought out.

INTRODUCTION

To prevent density rise during long-pulse H-mode discharges in DIII-D, it is estimated that the particle exhaust must be approximately equal to the particle input from external fueling. In DIII-D, this corresponds to about 25 Torr•l/s. In the DIII-D advanced divertor configuration, a baffled chamber with its throat close to the outboard strike region of the plasma is provided to trap and pump a fraction of the particles (Fig. 1). Based on DEGAS calculations of the pressure buildup in this chamber, a pumping speed of ≥50,000 l/s is needed to achieve the desired particle exhaust [1]. However, the toroidal conductance of the baffle chamber, for a 1-m-long section, is only about 2000 l/s. The cross-sectional area of this toroidal chamber cannot be increased to improve the conductance because this would adversely affect the maximum capability for high-current plasmas. The small (8-in.-diam) ports also hinder external pumping. In-vessel pumping is therefore necessary to achieve the desired pumping speed.

Two types of in-vessel pumping are considered: (1) a special type of titanium getter pump, based on a design developed for Tore Supra applications [2], and (2) a cryocondensation pump. The former has the advantage of being able to operate in a high-temperature environment, but its pumping characteristics are affected by residual gases. Also, the filament used to evaporate the titanium determines the life of the pump. On the other hand, the cryocondensation pump has well-known and predictable pumping characteristics, high pumping speed, high capacity, and the ability to regenerate the pumped gases. However, the high-temperature environment, pressure ranges extending to milliTorr, and problems arising from pulsed magnetic fields in tokamaks make the design of such a pump quite challenging. In what follows we elaborate on the designs of these two pumps.

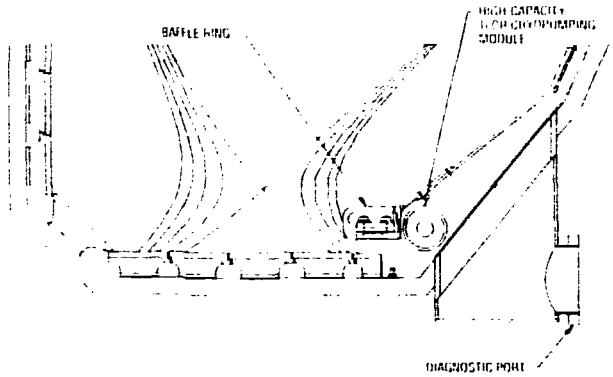

Fig. 1. Location of the baffle chamber and the pump in DIII-D.

TITANIUM GETTER PUMPS

In this scheme, several getter modules are distributed toroidally inside the baffled chamber to provide pumping. Each module consists of a stack of disks on which titanium is deposited with a filament running axially along the disks (Fig. 2). Following the prescriptions in Ref. [2], a thick coating of titanium (about 5000 monolayers or 1.7

*Research sponsored by the Office of Fusion Energy, U.S. Department of Energy, under contract DE-AC05-84OR21400 with Martin Marietta Energy Systems, Inc.

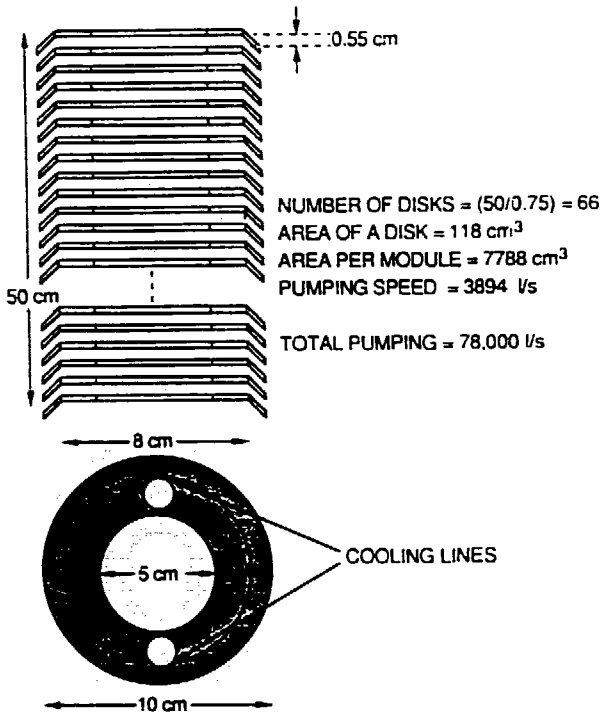

Fig. 2. Schematic of a getter pump module.

μm) is evaporated from the filament onto the disks. The outer diameter of the disks is selected on the basis of available space in the getter chamber and is 10 cm in our preliminary design. The disks are bent at an angle θ to prevent titanium from escaping the getter stack. This angle is also affected by the spacing between the disks; the closer the disks, the greater the angle and therefore the lower the probability of a gas particle finding its way to the titanium-coated surface. Another consideration is the variation in coating thickness. This variation increases as the disk spacing is reduced and decreases as the inner diameter of the disks is increased. The angle that corresponds to the condition where there is no line of sight to the filament is

$$\tan\theta = (R_3 - R_2)d/[(R_4 - R_3)(R_3 - R_2)] ,$$

where R_2 is the internal radius of the disk, R_3 is the radius where the disk is bent, R_4 is the external radius, and d is the disk gap.

The ratio of titanium deposited at R_3 to that at R_2 is

$$Q_3/Q_2 = (R_2/R_3)\,(1 - 1/\{1 + [d/(R_3 - R_2)]^2\}^{0.5}) .$$

A Monte Carlo code is being used to optimize the angle θ and the spacing between the disks.

For proper coating and to prevent overheating of the array, the disks are cooled during evaporation. Degassing is done by turning off the cooling and using the same filament to bake the disks to about 400°C for about 1 h [2].

The pumping characterization performed by the Tore Supra group was limited to pressures lower than 10^{-5} torr. We have measured the pumping speed at higher pressures by applying a thick coating (0.9 μm) on the inner surfaces of a stainless steel chamber with a volume of 6.3 l and a surface area of 2000 cm^2 under ultrahigh-vacuum conditions. The results are shown in Fig. 3. A pumping speed of about 1.5 $l \cdot s^{-1} \cdot cm^{-2}$ can be realized even at pressures approaching 1 mTorr. At the end of this experimental run, the gettered surfaces were left under vacuum (8.8×10^{-9} Torr) over the weekend. Measurements carried out after about 70 h showed that the pumping speed was reduced by a factor of about 20. This reduction in pumping performance is attributed to poisoning by residual gases present in the ultrahigh-vacuum chamber. Similar effects were reported by Druaux and Sledziewski [2], who also claim that the full pumping speed can be regained by applying a thin coat of titanium (about 200–300 monolayers) after degassing the disks. However, our attempt to rejuvenate the pumping characteristics of the thick layer mentioned above was only partially successful. The pumping speed measured after applying a thin coating of about 300 monolayers, following overnight baking at temperatures up to 370°C, decreased steadily with hydrogen loading (Fig. 4).

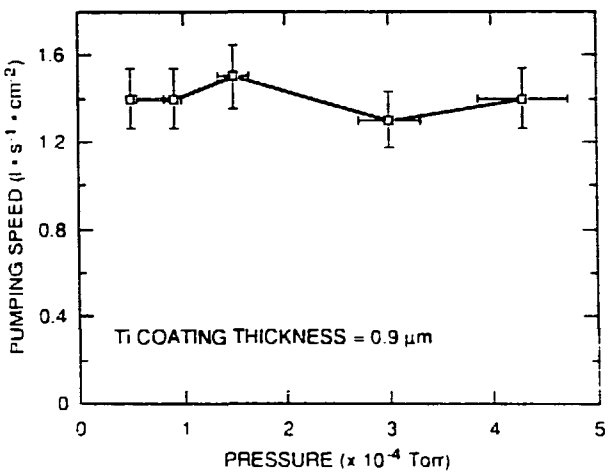

Fig. 3. Pumping speed vs pressure for a thick (0.9-μm) titanium layer.

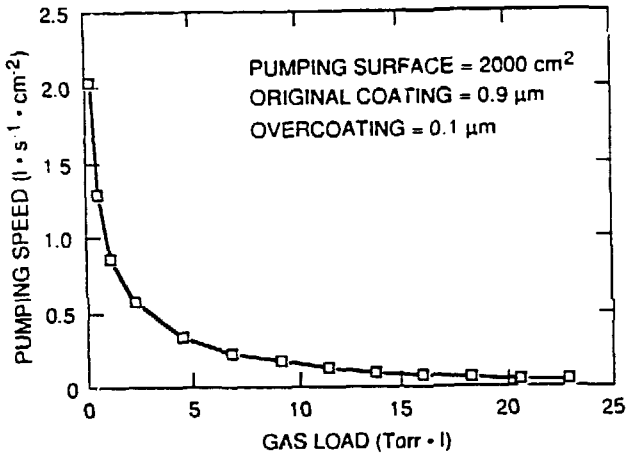

Fig. 4. Pumping speed vs hydrogen loading after poisoning and rejuvenation.

CRYOCONDENSATION PUMP

With a cryocondensation pump, the pumping surface is at liquid helium temperature, where the sticking coefficient for all gases except helium is close to unity. The pumping speed is reduced by the liquid-nitrogen-cooled chevron around the helium line. In our reference design, we consider a coaxial arrangement because of its simplicity. A standard 90° chevron spaced to provide no direct line of sight to helium cuts down the pumping speed of a bare helium panel by a factor of 4. Thus, a pumping speed of about 6 $l \cdot s^{-1} \cdot cm^{-2}$ can be realized for deuterium. The toroidal span for DIII-D is about 10 m. Therefore, a liquid-helium-cooled surface of about 10,000 cm^2 should provide the desired pumping of >50,000 l/s.

A variety of configurations can be envisioned for such a pump, and the search for an optimal geometry is under way. However, we base our analysis on the simple coaxial geometry shown schematically in Fig. 5. The heat loading from various factors obtained in this geometry can readily be applied to any other optimized configuration.

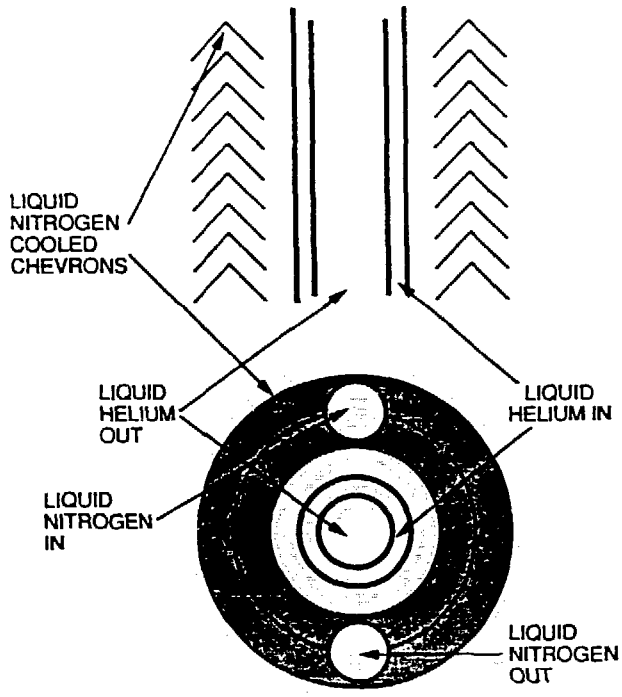

Fig. 5. Schematic of a cryocondensation pump.

Heat Loading on the Helium Line

1. Radiation load: For two concentric cylinders with an outer surface area A_2 at temperature T_2 and an inner surface area A_1 at temperature T_1, the radiation Q to the inner cylinder is

$$Q/A_1 = \sigma_S \left(1/\{(1/\varepsilon_1) + (A_1/A_2)[(1/\varepsilon_2) - 1]\} \right) (T_2^4 - T_1^4),$$

where $\sigma_S = 5.7 \times 10^{-12}$ W/cm^2 is the Stefan-Boltzmann constant, and ε_1 and ε_2 are the emissivities of the two surfaces. For $\varepsilon_1 = \varepsilon_2 = 1$ and $A_1 = A_2$,

$Q/A_1 = 46$ mW/cm^2 for $T_2 = 300$ K, $T_1 = 77$ K,
$= 200$ μW/cm^2 for $T_2 = 77$ K, $T_1 = 4.2$ K.

Thus, the total radiation load to the 10,000-cm^2 helium surface is 2 W.

2. Conduction heat load: This is heat transferred from the liquid nitrogen surface to the liquid helium line by way of solid supports and fittings. The exact magnitude depends on the details of the design. The heat conducted from a surface at T_2 to a surface at T_1 through a body of uniform cross section and length L is given by

$$Q = (A/L) \int \kappa \, dT$$

For stainless steel, κ varies from 2.5×10^{-3} W/cm•K at 4 K to 7.0×10^{-2} W/cm•K at 77 K. For example, the heat leak to the helium line from the nitrogen surface through a 1-cm-wide, 2-cm-long, 1-mm-thick

stainless steel strip is about 0.25 W. Thus, by clever design, it should be possible to support the helium line with a heat leak of less than 5 W. The end fittings usually contribute a few more watts.

3. Particle load: If we assume complete thermalization of all the particles to liquid nitrogen temperature, for a pulsed load of 25 Torr•l/s lasting for 4 s, there is a total of 100 Torr•l of gas or 3.6×10^{21} particles. The heat load per pulse is then 3.6×10^{21}[(3/2)kT + the latent heat of fusion per particle], where T is 77 K (the boiling point of liquid nitrogen). This heat load amounts to about 4 W/pulse. In practice, the assumption of complete thermalization of all particles to 77 K is not realistic. Moreover, a significant number of plasma particles at energies of a few electron-volts actually strike the liquid nitrogen shield. The increase in heat loading from these particles has been estimated in a DEGAS calculation, and the contribution to the liquid helium surface is between 2 and 20 W [3]. The wide range in this number arises from uncertainities in the reflection models of particles at energies of a few electron volts.

4. Heat loading due to eddy currents: This is dependent on the surface area and thickness of the helium line and the rate of change of the magnetic field. For a wire of radius R,

$$P_e = (\pi R \dot{B})^2/4\rho ,$$

which, when extended to a tube with outer and inner radii R_o and R_i, is given by

$$P_e = \pi^2 \dot{B}^2(R_o^2 - R_i^2)/4\rho$$

(in W/m^3) where $\dot{B}$ is the rate of change in the magnetic field (in Wb/m^2) and ρ is the resistivity (in Ω•m). Thus, the total eddy losses are estimated to be only 377 mW for a 10-m-long, 3-cm-diam stainless steel line with 1-mm-thick walls.

5. Induced voltage-driven load: If the cryogenic line has no insulating break, the voltage induced in the loop by the changing magnetic field will drive a current, thereby providing a heat load to the line. The loop voltage is decided by the operating conditions and can be up to 15 V in DIII-D. For a 10-m-long, 3-cm-diam stainless steel line with 1-mm-thick walls, the resistance is 40 mΩ. The power dissipation due to induced voltage in the loop can thus be up to 250 W. If a single loop is used, the line should be provided with insulating breaks.

6. Electron cyclotron heating (ECH) load: The power absorbed by a metal surface, assuming isotropic radiation, is

$$P_{abs} = P_o(8R_sA_s/3\eta),$$

with $R_s = (\pi f\mu/\sigma)^{1/2}$, where f is the frequency (s^{-1}), $\mu = 4\pi \times 10^{-7}$ H/m is the free-space permittivity, σ is the conductivity (mho/m), A_s is the surface area, η is 377 Ω, and P_o is the power incident on the surface. Only about 10% of the ECH power will be dissipated on the walls, since plasma is a good absorber, and only a small fraction of this power will enter the baffle chamber. Some of the power that enters the baffle chamber will be absorbed by the helium line. An exact calculation is difficult because of the multiple reflection at the walls, escape of energy through the windows of the vacuum vessel, etc.; a very crude estimate gives a power of less than 4 W for 2 MW of ECH power.

7. Neutron loading: If the neutron production rate is 10^{15} s^{-1}, the neutron loading on the helium line is less than 10 mW for a 3-cm-diam line with a surface area of 10,000 cm^2.

Heat Loading on the Liquid Nitrogen Circuit

If the baffle plate is not water cooled and its temperature reaches 200°C, then the radiation load to the nitrogen line is by far the main contributor and is about 2.8 W/cm^2.

Other Design Considerations

1. Glow discharge cleaning of the tokamak: The DIII-D tokamak operating scenario involves helium glow discharge cleaning between shots. The pressure during glow is typically 2 mTorr, and it is hoped to operate at a reduced pressure of 1 mTorr with electron-assisted glow. We can calculate the arrival rate to be 3.5×10^{22}[p/(MT)$^{0.5}$] per square centimeter (for p in Torr). If the helium gas at T_i is

completely thermalized to liquid nitrogen temperature T_2, the pressure inside the nitrogen surface is

$$p_1/p_2 = (T_1/T_2)^{0.5} .$$

Thus, the arrival rate at the liquid helium surface is

$$3.5 \times 10^{22}[p_1(T_2/T_1)^{0.5}/(MT_2)^{0.5}] = 3.5 \times 10^{22}\,[p_1/(MT_1)^{0.5}] .$$

For p = 1 mTorr, the arrival rate is 9.8×10^{17} He molecules/cm^2-s, and the heat input to the helium is equal to the arrival rate times 1.5kT, which is 1.56 mW/cm^2-mTorr. Thus, for a line with an area of 10,000 cm^2, the heat loading during a helium glow discharge at 2 mTorr could be 31.2 W, lasting for several minutes. In practice, this figure will be higher, because our assumption of complete thermalization of all particles to 77 K is not realistic for normal types of chevrons.

A more serious thermal load to the helium line occurs during the helium gas filling to initiate the glow. In present experiments, the pressure is raised instantaneously to 50 mTorr; when the discharge strikes, it is brought down with an e-folding time of 10 s. Based on the rate of 15.6 W/mTorr, we can see the equivalent of a few hundred watts of heat loading lasting for a few seconds. Moreover, since the mean free path of helium at 50 mTorr is only 2.6 mm, many particles at the baffle wall temperature will find their way to the helium line without impinging on the nitrogen chevron, thereby increasing the heat input by a factor of about 5. This heat load of about 1 kW to the helium line lasting for a few seconds will be the determining factor in the design of the cryogenic loop.

2. Disruption forces on the cryopump: These forces arise from the interaction of currents induced in the line with the magnetic field perpendicular to it ($\mathbf{J} \times \mathbf{B}$ force). An estimate of the force would require details of the disruption conditions and of the pump.

ACKNOWLEDGMENTS

The authors are grateful for help provided by J. E. Simpkins during gettering experiments. Discussions with P. Bonnel, D. Hill, G. Jackson, A. Langhorn A. Mahdavi, M. Schaffer, and M. Tupper were quite valuable.

REFERENCES

[1] L. W. Owen and P. K. Mioduszewski, Oak Ridge National Laboratory, personal communication, 1989.

[2] Z. Sledziewski and J. Druaux, "Titanium Getter Pumps for the Tore Supra Neutral Beam Lines," in *Fusion Technology 1986: Proceedings of the 14th Symposium*, Avignon, 1986, vol. 1, pp. 533–38.

[3] L.W. Owen and P. Mioduzewski, unpublished.

DISCLAIMER